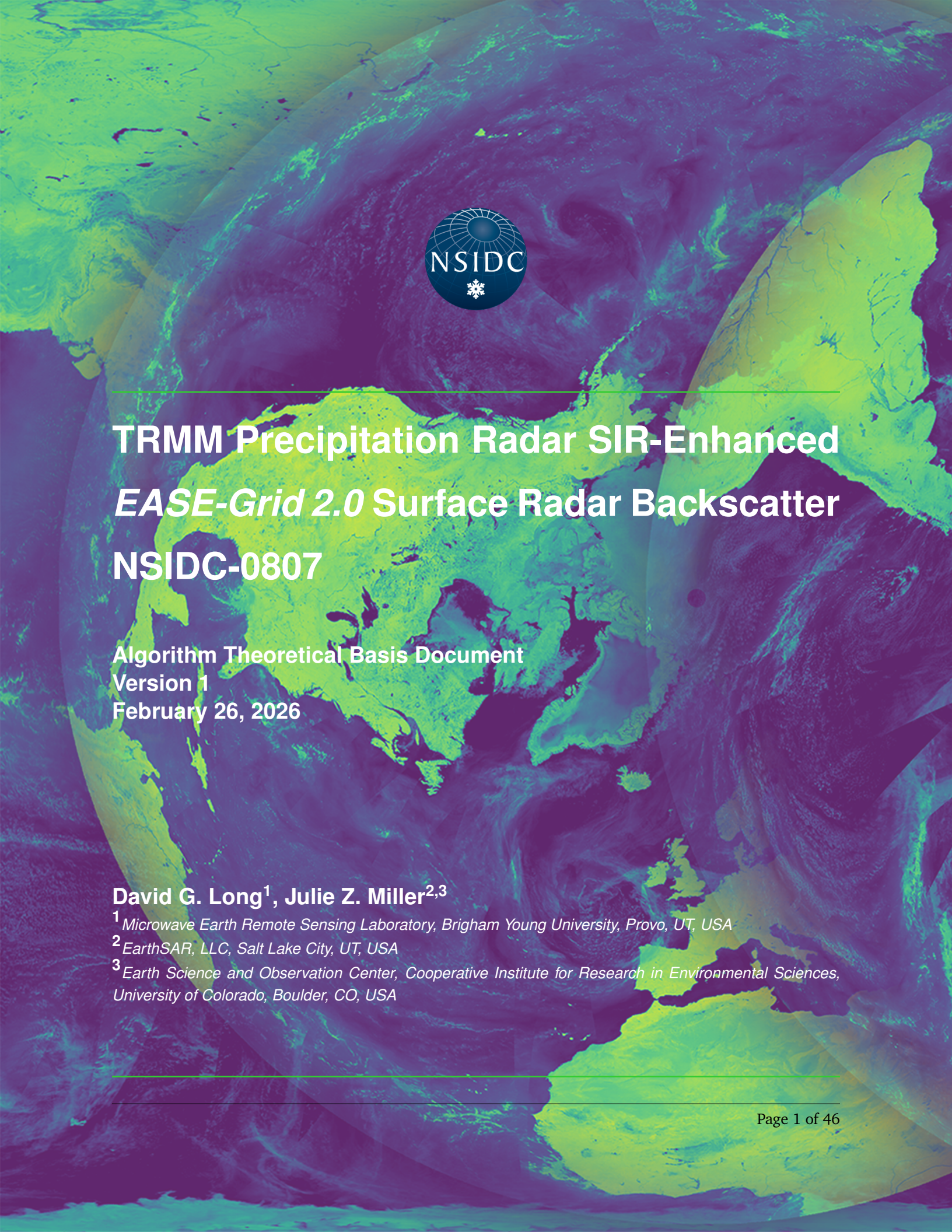

TRMM Precipitation Radar SIR-Enhanced *EASE-Grid 2.0* Surface Radar Backscatter NSIDC-0807

Algorithm Theoretical Basis Document
Version 1
February 26, 2026

David G. Long[1], Julie Z. Miller[2,3]

[1] *Microwave Earth Remote Sensing Laboratory, Brigham Young University, Provo, UT, USA*

[2] *EarthSAR, LLC, Salt Lake City, UT, USA*

[3] *Earth Science and Observation Center, Cooperative Institute for Research in Environmental Sciences, University of Colorado, Boulder, CO, USA*

Cover Image
Color montage of morning overpass AMSR2 horizontally-polarized 36 GHz passive microwave brightness temperatures, 29–30 June, 2003, by M. J. Brodzik, National Snow and Ice Data Center.

Citation
David G. Long & Julie Z. Miller. 2024. TRMM Precipitation Radar SIR-Enhanced EASE-Grid 2.0 Surface Radar Backscatter Algorithm Theoretical Basis Document, Version 1.0. NSIDC White Paper. https://doi.org/10.5281/zenodo.14582576.

Contents

List of Figures

List of Tables

1 Revision History

Table 1: *ATBD Revision History*

Revision	Date	Purpose
1.0	2026-02-26	Initial Version

Table 2: *Data Set Revision History*

Revision	Date	Purpose
1.0	2026-02-26	Initial Data Release

2 Acronyms and Abbreviations

Table 3: *List of Acronyms and Abbreviations*

ATBD	Algorithm Theoretical Basis Document
AVE	weighted AVEraging image formation algorithm
CDR	Climate Data Record
CETB	Calibrated Passive Microwave Daily EASE-Grid 2.0 Brightness Temperature
DAAC	Distributed Active Archive Center
dB	decibel ($10\log_{10}$)
DIB	Drop-In-the-Bucket averaging (used to produce GRD products)
DOY	Day Of Year
EASE-Grid	Equal-Area Scalable Earth Grid (Original Definition)
EASE-Grid 2.0	Equal-Area Scalable Earth Grid Version 2.0
EASE2-M	EASE-Grid 2.0, Mid- and Low-Latitude Cylindrical Projection
EASE2-N	EASE-Grid 2.0, Northern Hemisphere Projection
EASE2-S	EASE-Grid 2.0, Southern Hemisphere Projection
EASE2-T	EASE-Grid 2.0, Temperate and Tropical Cylindrical Projection
EOSDIS	Earth Observing System Data and Information System
ESDR	Earth System Data Record
GHz	GigaHertz
GRD	(Drop-In-the-Bucket) Gridding Method
HH	Horizontal-polarization transmit, Horizontal-polarization receive
MEaSUREs	Making Earth System Data Records for Use in Research Environments
MRF	Measurement Response Function
NASA	National Aeronautics and Space Administration
NSIDC	National Snow and Ice Data Center
NetCDF	Network Common Data Format
PR	Precipitation Radar
PSRF	Pixel Spatial Response Function
SCP	Scatterometer Climate Record Pathfinder
Sigma-0	normalized radar cross section or backscatter (σ^o)
SIR	Scatterometer Image Reconstruction
TRMM	Tropical Rain Measuring Mission
UTC	Coordinated Universal Time
VV	Vertical-polarization transmit, Vertical-polarization receive

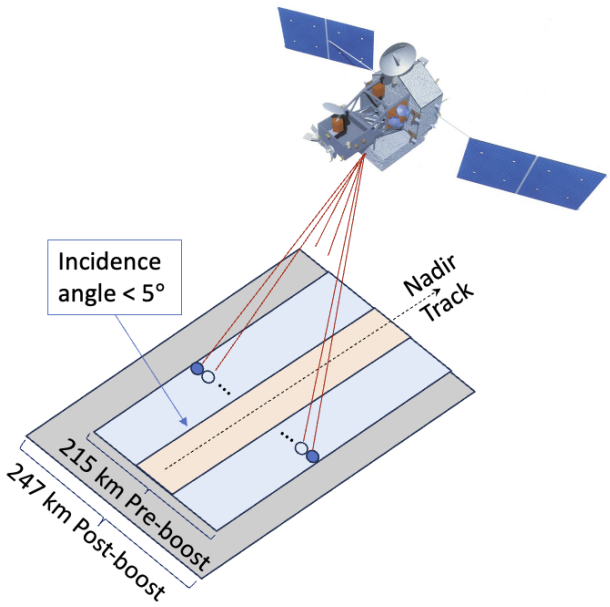

Figure 1: *TRMM PR observation swath. Nominally 5 km σ^o measurements are collected over a 215 km pre-boost and 247 km post-bost swath with incidence angles between 0–17° pre-boost and 0–18° post-boost (Kozu et al., 2001)(Team, 2011a). The σ^o measurements within the inner swath have incidence angles less than 5°.*

3 Purpose of this Document

This document describes a CETB-compatible radar backscatter product created from TRMM PR 13.88 GHz radar observations of the surface backscatter collected during the TRMM mission in 1997–2014. Originally, TRMM was operated in a 350 km high orbit, but in Aug 2001, the orbit was boosted to 402 km altitude in order to extend the mission life. This had the effect of increasing the swath width and incidence angle range of the PR. During the pre-boost period (1997–2001) the TRMM PR (Kozu et al., 2001) collected nominally $\sim$5 km resolution normalized radar cross section (σ^o) over a narrow 215 km wide swath, see Fig. 1 (Kozu et al., 2001)(Kawanishi et al., 2000). Post-boost, the swath width was 247 km.

Although designed and optimized for rain observation, TRMM PR also collected surface σ^o measurements over land within $\pm 66°$ latitude. This includes some glaciated regions. The observed σ^o depends on the surface roughness, geometry, and dielectric constant. These depend on geophysical parameters of interest such as surface freeze/thaw state, snow and ice structure, moisture content, and vegetation characteristics, among others (Ulaby and Long, 2014). The TRMM PR data set provides a unique “snapshot” of the Earth during its mission lifetime.

The TRMM PR radar backscatter (*TRMM PR*) product exploits the TRMM PR measurements to create a unique backscatter image data set that captures the state of the Earth during the TRMM PR mission (1997-2014). To exploit this data, we employ image reconstruction techniques to create conventional resolution and enhanced resolution TRMM PR radar images from the measurements. The new data set is provided to the science community to support cryosphere and climate studies.

4 Gridded and SIR-Enhanced Product Description

4.1 Product Description

The *TRMM PR* product includes Level 3 gridded radar backscatter data collected at 13.88 GHz with horizontal transmit-horizontal receive (HH) polarization. Data are gridded to the EASE-Grid 2.0 Cylindrical projections (Brodzik et al., 2012)(Brodzik et al., 2014), at two spatial resolutions, as described below. The *TRMM PR* product is archived and distributed by the National Snow and Ice Data Center Distributed Active Archive Center (`https://doi.org/10.5067/WK4DZ1LG4L6O`).

Input data for the *TRMM PR* v1.0 product are the TRMM PR 2A21 Version 7 files obtained from the NASA EOSDIS system. The data coverage is global for the period beginning 1 January 1998 through the 7 October 2014 – the full mission lifetime. No calibration corrections have been applied to the data.

4.2 TRMM PR Instrument

TRMM PR flew as a primary payload on the TRMM mission (Simpson et al., 1988) launched in 1997. The TRMM PR instrument is described in Kozu et al. (2001), Kawanishi et al. (2000), Team (2011b). TRMM PR is a fan-beam Doppler range-gate scatterometer that uses pulse compression to achieve range resolution. The TRMM PR instrument employs a unique antenna configuration that provides multiple pencil beams that collected measurements across a narrow swath centered around the nadir track. The incidence angle of the observations span -18° to 18° where the negative incidence angle refers to one side of the swath and the positive values to the other side of the swath, see Fig. 1. Along-track and cross-track resolution is provided by the narrow beamwidth of the antenna beams.

Multiple pulses are processed and summed into a single measurement. The SRF of an individual σ^o measurements is effectively defined by the antenna gain pattern[1]. TRMM PR collected return echo power measurements, which were converted into σ^o using the radar equation (Team, 2011b)(Ulaby and Long, 2014). The σ^o value depends on the surface roughness, geometry, and dielectric constant (Ulaby and Long, 2014). As described below, from these σ^o measurements global images were created by (1) DIB gridding of the σ^o measurements on a 25 km grid and (2) applying the AVE algorithm on a 3.125 km grid.

[1]Note that while a radiometer's footprint is defined by the antenna pattern, the radar footprint is defined by the antenna pattern squared due to the two-way travel of the signal from radar to the surface and back, by range-gate timing, and by signal processing of the signal (Ulaby and Long, 2014).

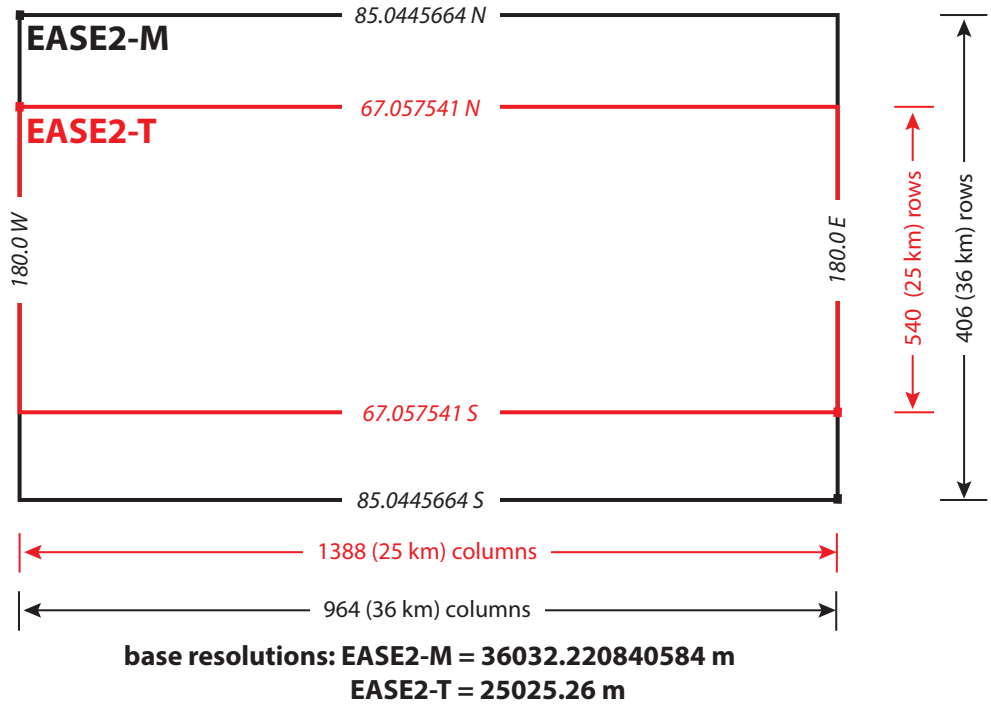

Figure 2: *Relationship of EASE-Grid 2.0 cylindrical projection extents. The EASE2-T extent is defined for compatibility with other CETB products. The difference in latitudinal extent is exaggerated (Brodzik et al., 2021).*

4.3 Grid Spatial Extent

The spatial extent of the equal-area cylindrical projection (Fig. 2) is defined to match the extent of compatible grids favored by two user communities: (1) the Mid-Latitude (EASE2-M) grid, extending to $\pm 85.0445664^\circ$ latitude, has been adopted by the SMAP user community. And, (2) the Temperate and Tropical (EASE2-T) grid, limited to latitudes equatorward of $\pm 67.1^\circ$, is consistent with the original CETB products defined for similar scanning radiometers (Brodzik et al., 2021). See Appendix A Table 6 for grid specifications.

4.4 Grid Spatial Resolution

TRMM PR grid resolutions are defined relative to a 25 km base resolution, i.e., 25 km and 3.125 km MEaSUREs CETB data products (Brodzik et al., 2021). Nested resolutions relative to the CETB 25 km base grids are defined using exact divisors of 2, as illustrated in Figure 3. *TRMM PR* projection extents, dimensions and grid cell size details are included in Appendix A. Grids used for *TRMM PR* processing are included in Table 4.

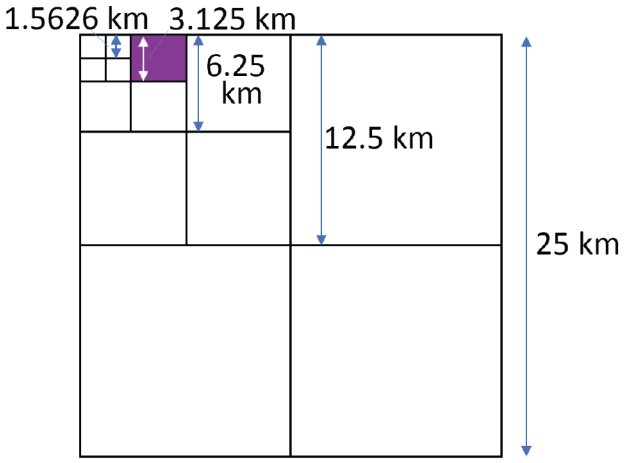

Figure 3: *CETB nested grids based on a 25 km base resolution. Only 25 km and 3.125 km divisions are used for the* TRMM PR *products (Long et al., 2019).*

Table 4: TRMM PR *EASE-Grid 2.0 base grids produced by the projection and reconstruction algorithm for the TRMM PR product.*

EASE2-M	EASE2-N	EASE2-S	EASE2-T
n/a	n/a	n/a	25km (GRD)
n/a	n/a	n/a	3.125km (AVE)

4.5 Data Products

The *TRMM PR* product at the NSIDC DAAC covers the period beginning 1 Jan 1998 through 2014 (DOY 247). No calibration corrections have been applied to the data. In creating a time series, a "moving average" approach is used with overlapping imaging periods that start on a mission day and extend through the 28-day period (or to the end of the mission, whichever comes first) starting at 14 day intervals. Table 5 summarizes the available *TRMM PR* products, which are all in CETB-standard EASE-2 Grid projections.

Table 5: *Available TRMM PR Image Products. TRMM PR operates at VV polarization.*

Image Period	Algorithm	Pix. Res. (km)	Regions*	Size T (MB)
28 days	GRD	25	T	3.6
28 days	AVE	3.125	T	190

∗ Region code: T=Global

5 Algorithm Description

5.1 Background

The *effective resolution* of an image is defined by the *pixel spatial response function* (PSRF), where the effective resolution is given by the dimension(s) of the one-half power (3-dB) extent of the PSRF. In contrast, the *measurement response function* (MRF) describes the spatial characteristics of the *individual* measurements that were combined to create the image. For a radar, the MRF depends on the two-way antenna gain pattern, the scan geometry, and the signal processing. For both radars and radiometers, the PSRF depends on the MRF and the image formation algorithm. In a linear image formation algorithm, the reported pixel value consists of the weighted sum of nearby measurements. In this case the PSRF is then the normalized weighted sum of the measurement MRF functions, including their spatial offset from the center of the pixel.

The spacing of pixels is termed the "pixel posting" or the "posting resolution". In creating the *TRMM PR* backscatter image product, multiple measurements from different passes are combined into single pixel values. The resulting image pixels have an effective resolution slightly coarser than the posting resolution since (1) the measurements are not all centered the same, and (2) their MRFs can extend outside of the pixel area. The PSRF provides the tool for defining the effective pixel resolution (Long and Brodzik, 2016a). In order to be compatible with the CETB data set, two posting resolutions are considered: 25 km and 3.125 km, see Fig. 4. The former is used only for gridded (DIB) products while the latter is used for enhanced resolution products such as AVE and SIR, though the TRMM PR product does not use SIR.

5.2 *TRMM PR* Backscatter Image Products

The *TRMM PR* backscatter products include both low-noise (low-resolution) coarse resolution GRD images and higher-noise (enhanced) fine-resolution (AVE) images. The various products have their advantages and disadvantages. Multiple image types allow users the flexibility of choosing the appropriate images for their research application.

To create radar CETB-compatible products, different approaches are used for each resolution. With the PR's narrow swath, In order to estimate the incidence angle dependence in each pixel, multiple passes over an extended imaging period are required. While TRMM had a 42 day repeat cycle, this is considered excessive, so the shortest imaging period that provided sufficient repeat pass coverage was selected. This is a 28 day imaging period with 50% overlap of the imaging periods. The 28 day period is recognized to be rather long, but is required for the required overlap.

For GRD images, the source backscatter measurements are gridded onto a 25 km grid using DIB techniques. In this approach, all the measurements whose center location falls

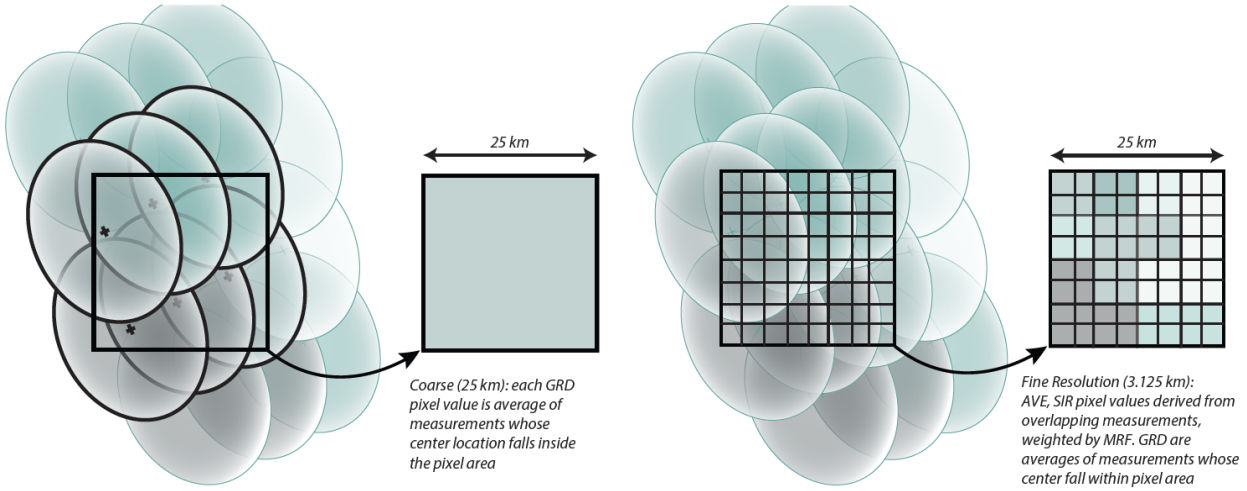

Figure 4: *Conceptual illustration of coarse 25 km (left) vs. high resolution 3.125 km (right) pixels. The ellipses represent the individual MRFs of the measurements (the actual shapes are more complicated than this.) DIB is used for GRD images while AVE and SIR are used for high resolution images.*

within a grid element are averaged into the reported value. For the 3.125 km product, the source measurements are processed using the the first iteration of the SIR algorithm, termed 'AVE'. AVE images are weighted averages of the measurements which cover the pixel, where the weighting is based on the measurement MRF, which varies from measurement to measurement. Table 5 summarizes the image product types. Only AVE images are producted for the TRMM PR product.

5.3 Radar Spatial Response and Image Reconstruction

The effective spatial resolution of an image product is determined by the MRF of the sensor and by the image formation algorithm used. As previously noted, the MRF is determined by the antenna gain pattern, the scan geometry (notably the antenna scan angle), and the signal processing, see Long et al. (1993), Long (2017), Lindsley et al. (2016), Long and Brodzik (2016a). The goal in forming a σ^o image is to estimate the backscatter properties of the surface from noisy measurements that employ (possibly variable) MRFs that sample the surface. Though simple to implement, DIB techniques ignore the MRF, which limits their effective resolution. Reconstruction techniques that use the MRF can provide much finer effective resolution.

Reconstruction processing techniques effectively assume the underlying signal (the backscatter) being sampled is band-limited, which is the only consistent assumption possible with sampled data (Long and Brodzik, 2016b, Long and Franz, 2016b). For reconstruction, the backscatter at each point of a fine-scale pixel grid is estimated, producing a backscatter

image or map. While the image is generated on a regular grid, the measurement locations and MRF are not aligned with the grid, and so the measurements form an irregular sampling pattern, which can complicate signal reconstruction. Many commonly used image formation algorithms either ignore this (as is done in DIB) or attempt to interpolate or distance-weight the measurements values. In using image reconstruction, we avoid these ad hoc, non-optimal approaches and explicitly compute the MRF of each measurement as part of the reconstruction process. This is computationally intense, but provides the best possible image construction. The remainder of this section outlines this process.

An individual scatterometer backscatter measurement z_i can be modeled as the integral of the product of the MRF and the surface backscatter, i.e.,

$$z_i = \iint \text{MRF}_i(x, y; pp)\sigma^o(x, y, \theta, \phi_i, t, pp)dxdy + \text{noise} \tag{1}$$

where $\text{MRF}_i(x, y; pp)$ is the spatial MRF of the ith measurement at x, y and the surface σ^o depends on spatial location x, y, incidence angle θ, azimuth angle ϕ, time t, and polarization pp, i.e.,

$$\text{MRF}_i(x, y; pp) = \iint \frac{G_a^2(x, y; pp)G_p(x, y; pp)}{R^4(x, y)}. \tag{2}$$

where

$$X = \iint \frac{G_a^2(x, y; pp)G_p(x, y; pp)}{R^4(x, y)}dxdy. \tag{3}$$

where $G_a(x, y; pp)$ is the effective two-way antenna gain at the surface at (x, y) for polarization pp, $G_p(x, y; pp)$ is the processor gain, and $R(x, y)$ is the slant range from the radar to the surface. Note that the measurement is an average of σ^o in spatial coordinates as well as in azimuth and incidence angles.

Eq. 1 is discretized on the imaging grid to become

$$z_i = \sum_{j \in \text{image}} h_{ij}a_j + \text{noise} \tag{4}$$

where a_j is the backscatter at the center of the j^{th} pixel at (x_l, y_k) and $h_{ij} = MRF(x_l, y_k; \phi_i)$ is the discretely sampled MRF for the i-th measurement evaluated at the j-th pixel center where h_{ij} is normalized so that $\sum_j h_{ij} = 1$. In practice, the MRF is negligible some distance from the measurement center, so the sums need only be computed over a small area around the pixel. Ignoring the noise, Eq. 4 can be written as the matrix equation

$$\vec{Z} = \mathbf{H}\vec{a} \tag{5}$$

where $\mathbf{H}$ contains the sampled MRF for each measurement and $\vec{Z}$ and $\vec{a}$ are vectors composed of the measurements z_i and a_j, respectively. Even for small images, $\mathbf{H}$ is large and

sparse, and may be over-determined or under-determined depending on the number and locations of the measurements. Reconstruction of the surface σ^o is equivalent to inverting Eq. 5.

The iterative SIR algorithm (Early and Long, 2001)(Long et al., 1993) is a particular reconstruction algorithm that is specifically developed for scatterometer image formation. SIR approximates a maximum-entropy solution to an under-determined equation and a least-squares solution to an over-determined system. The first iteration of SIR is termed 'AVE' (for weighted AVErage) and provides a simple reconstruction estimate that is refined in later SIR iterations. The AVE estimate of the j-th pixel is given by

$$a_j = \frac{\sum_i h_{ij} z_i}{\sum_i h_{ij}} \tag{6}$$

where the sums are over all measurements that have non-negligible MRF at the pixel. The SIR iteration begins with an initial image a_j^0 whose pixels are set to the AVE values defined in Eq. 6. Thereafter, the iterative equation for single-variate SIR is given by

$$a_j^{k+1} = \frac{\sum_i u_{ij}^k h_{ij}}{\sum_i h_{ij}} \tag{7}$$

where

$$u_{ij}^k = \begin{cases} \left[\frac{1}{2p_i^k}\left(1 - \frac{1}{d_i^k}\right) + \frac{1}{a_j^k d_i^k}\right]^{-1} & d_i^k \geq 1 \\ \frac{1}{2}p_i^k(1 - d_i^k) + a_j^k d_i^k & d_i^k < 1 \end{cases} \tag{8}$$

$$d_i^k = \left(\frac{z_i}{p_i^k}\right)^{\lambda} \tag{9}$$

where $d_i^k = (s_i/p_i^k)^{\lambda}$ with $\lambda = \frac{1}{2}$. The factor d_i^k is the square root of the ratio of a measurement to its forward projection at the k^{th} iteration. The update term u_{ij}^k is a non-linear function of both d_i^k and the previous image a_j^k. The sigmoid-like non-linearity in Eq. 8 constrains the amount of change permitted during any one iteration, thereby minimizing the effects of noise (Long et al., 1993). Though not used in this product, a spatial median filter can be applied to the image between iterations to further reduce the noise (Long et al., 1993).

For scatterometers, AVE and SIR are implemented in dB (Long, 2017)(Early and Long, 2001)(Long et al., 1993); i.e., the computation is done on $10\log_{10}(z_i)$ rather than on the linear-space value z_i as done in the radiometer version of SIR (Long and Brodzik, 2016a)(Long and Daum, 1998). In considering the differences between linear and dB processing, recall the well-known fact that computing the arithmetic mean of values in dB is equivalent to computing $10\log_{10}$ of the geometric mean of the linear-space values (Wikipedia, 2016).

With the measurements in dB, the reconstruction processing can be viewed as a form of weighted geometric mean filtering. Since it has been found that geometric mean filters are better at reducing Gaussian-type noise and preserving linear features than (linear) arithmetic mean filters (Pitas and Venetsanopoulos, 1986), some performance advantage to dB processing is expected and observed (Long, 2017). The linear and dB computations yield similar, but slightly different results, due to the varying signal-to-noise ratio (SNR) of the measurements and limited signal dynamic range (Long, 2017).

In practice, since the σ^o measurements are quite noisy, attempting full image reconstruction can produce excessive noise enhancement. In general, more iterations improve the signal and resolution, but also increase the noise level. To reduce noise enhancement and resulting artifacts, regularization can be employed, at the expense of resolution (Long and Franz, 2016a)(Early and Long, 2001)(Long et al., 1993)(Long, 2017). Regularization is a smoothing constraint introduced in an inverse problem to prevent extreme values or over-fitting. Regularization results in partial or incomplete reconstruction of the signal (Long and Franz, 2016a). It also creates a trade off between signal reconstruction accuracy and noise enhancement. SIR includes regularization achieved by prematurely terminating the iteration. We note that for a noisy sensor like a scatterometer, the results are not particularly sensitive to the precise value chosen, hence a fixed value can be selected. Selection of the number of iterations is based on simulation, see Early and Long (2001), Long et al. (1993) and Long (2017).

5.4 Sample Data

Figure 5 presents examples of 28-day product images with the gray scale set to emphasize the land σ^o . Swath-like artifacts are the result of temporal variations in the surface σ^o during the imaging interval. Since the images are created from measurements over extended periods, the ocean values are not considered particularly useful. Land and ice σ^o is much more stable and is the focus of this product. At the scale of Fig. 5, the differences between AVE and SIR images are not apparent. For this reason, only AVE images are available in the TRMM PR product. To better enable a comparison of the AVE and SIR images, see Figs. 6–9 which show zoom-in views of the Himalays region.

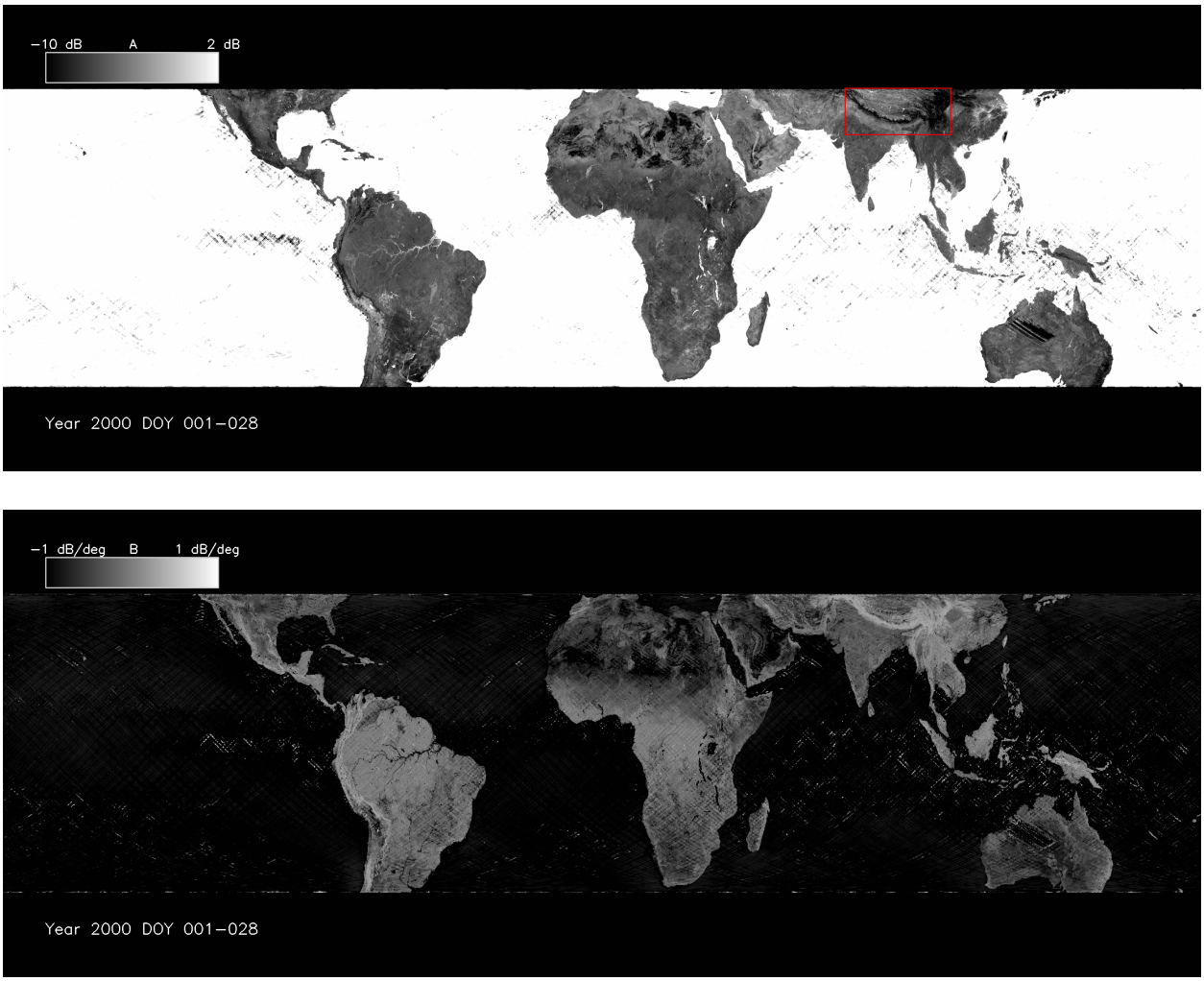

Figure 5: *Visualizations of examples of 28-day (DOY 1-28, 2000) TRMM PR (top) A (σ^o at 11° incidence angle) and (bottom) B (slope of σ^o versus incidence angle in dB/deg at 11° incidence angle) images. Images have been reduced in resolution for presentation here. Box shows study area in more detail in Figs. 6–9.*

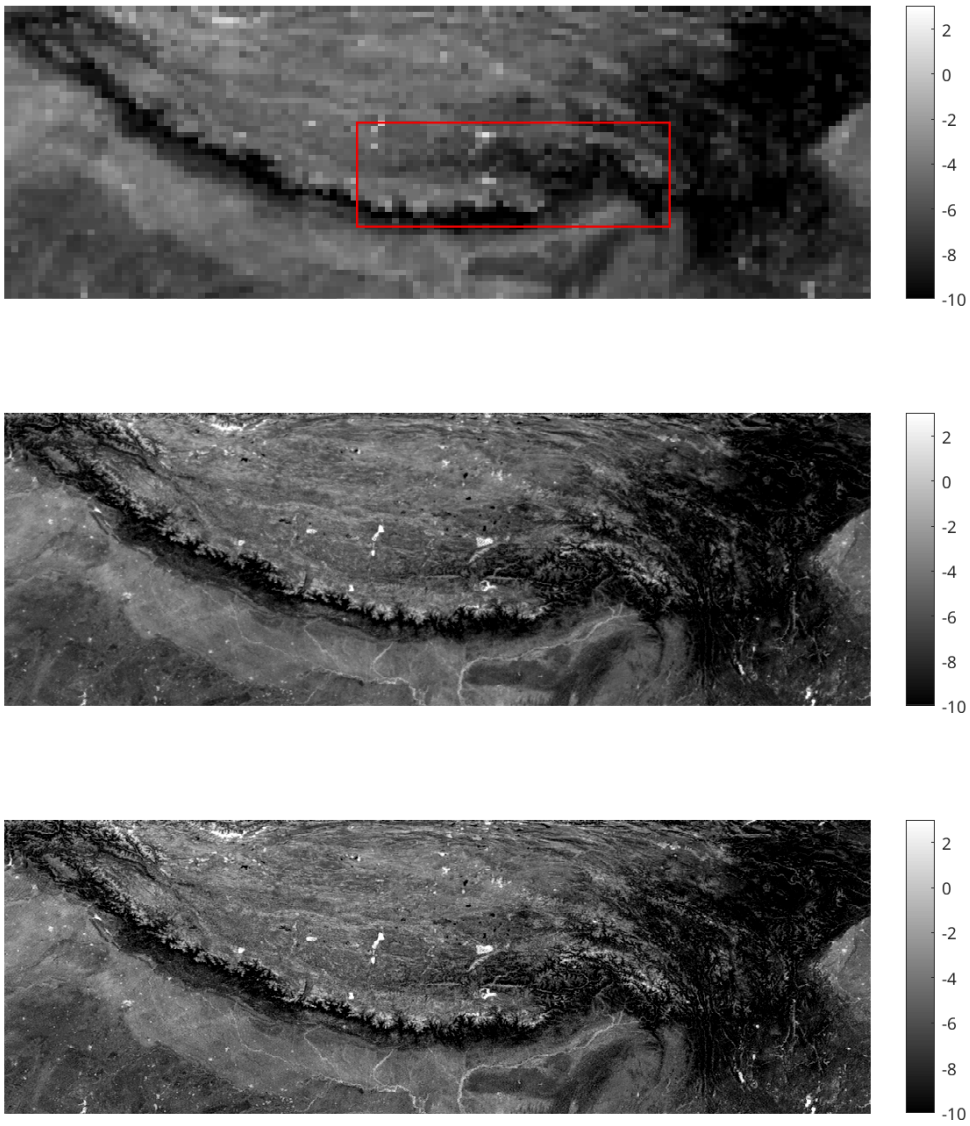

Figure 6: *Zoom-in of A images in the Himalayas study region to compare AVE and SIR images in Fig. 5.*

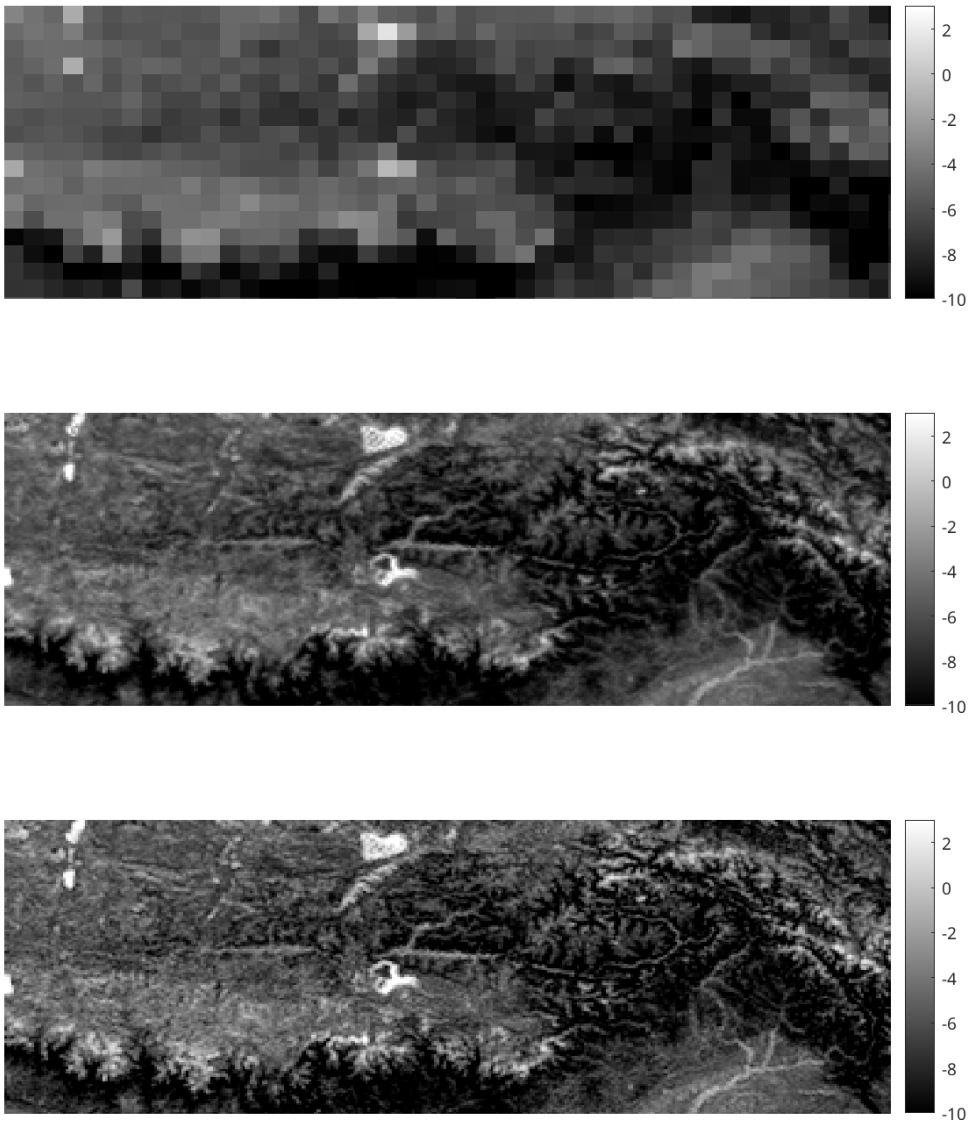

Figure 7: *Zoom-in of A images in the Himalayas study region to compare AVE and SIR images in Fig. 6.*

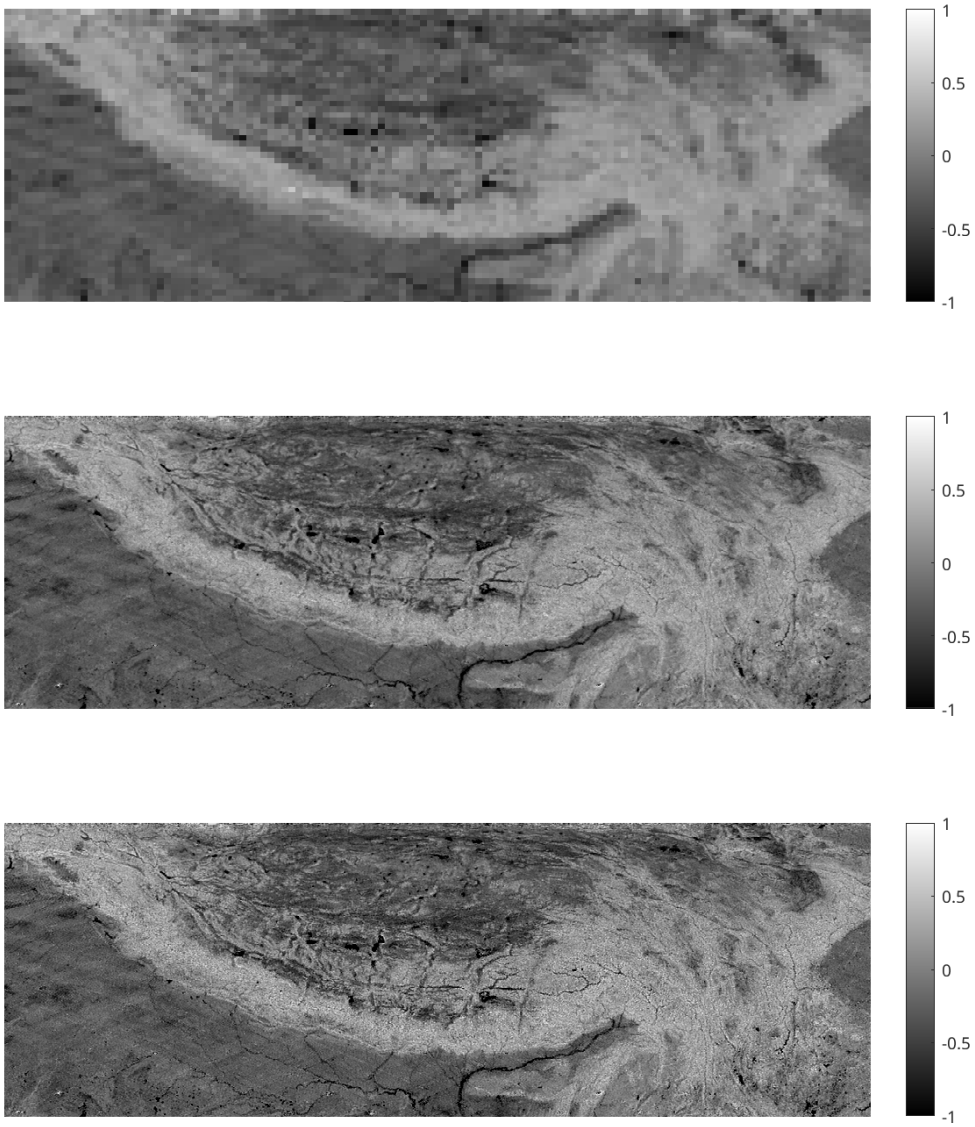

Figure 8: *Zoom-in of B images in the Himalayas study region to compare AVE and SIR images in Fig. 5.*

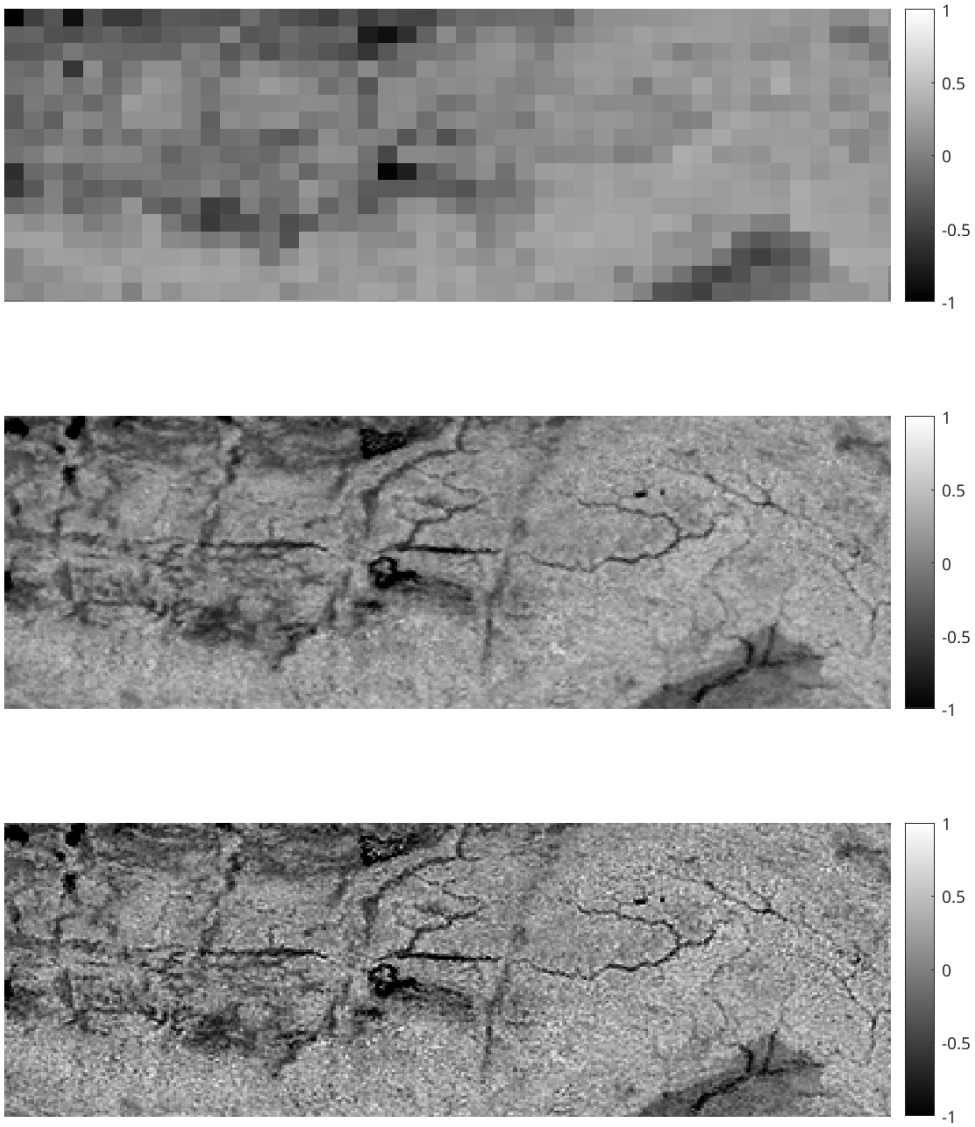

Figure 9: *Zoom-in of B images in the Himalayas study region to compare AVE and SIR images in Fig. 8.*

6 Measurement Modeling

6.1 Incidence Angle Effects

Over natural surfaces σ^o depends on the measurement incidence angle. Since TRMM PR is a fan-beam system, it collects σ^o measurements over a range of incidence angles ranging from about 15° to 60°. The variation in incidence angle must be accounted for when combining multiple measurements taken at different incidence angles. The incidence angle normalization $\gamma^o = \sigma^o / \cos\theta$ where θ is the incidence angle is sometimes used. However, the slope of this correction is strictly downward and since upward slopes are observed in some areas, this normalization is not used. Further, this normalization is based on specific backscatter model which does not apply to all natural surfaces. Instead, following prior investigators, see Long et al. (1993), Long and Miller (2023), Long and Miller (2024), and references therein, a linear slope is used that is centered at 11°, i.e., σ^o as a function of incidence angle is modeled according to

$$\sigma^o = A + B(\theta - 11^\circ) \tag{10}$$

where A is σ^o at 11° incidence angle; B is the slope of σ^o versus incidence angle θ. At each pixel, the model parameters A (the mean σ^o), B (the normalized slope of σ^o versus incidence angle) are estimated from the backscatter measurements on a pixel by pixel basis. The model parameters (A and B) are estimated only from measurements with incidence angles greater than or equal to 5°.

Figure 10 illustrates TRMM PR σ^o versus incidence angles at several arbitrary locations for Jan. 2000 days 1-28. Measurements as from 2° longitude by 1° latitude boxes with corners as indicated in the plot titles. Note the linear dependence of σ^o in dB with incidence angles for incidence angles greater than 5°. A linear fit of σ^o in dB versus incidence angle is shown, with the coefficients from Eq. 10 shown. Note that due to the curvature of σ^o versus incidence angle for measurements with incidence angles less than 5°, measurements with incidence angles less than 5° were not included in the linear fit.

6.2 Temporal Sampling

The variation in σ^o as a function of azimuth and incidence angles for different measurements is important and provides useful geophysical information. Incidence angle variation is considered in the previous section.

Unfortunately, the TRMM PR measurement sampling does not fully cover the surface in a single pass, i.e., the surface is undersampled, so there are areas of pixels with only a single measurement available. For this case, the AVE image can only report this measurements' value over the area of its non-zero MRF and it is impossible to compute the B value for the pixel.

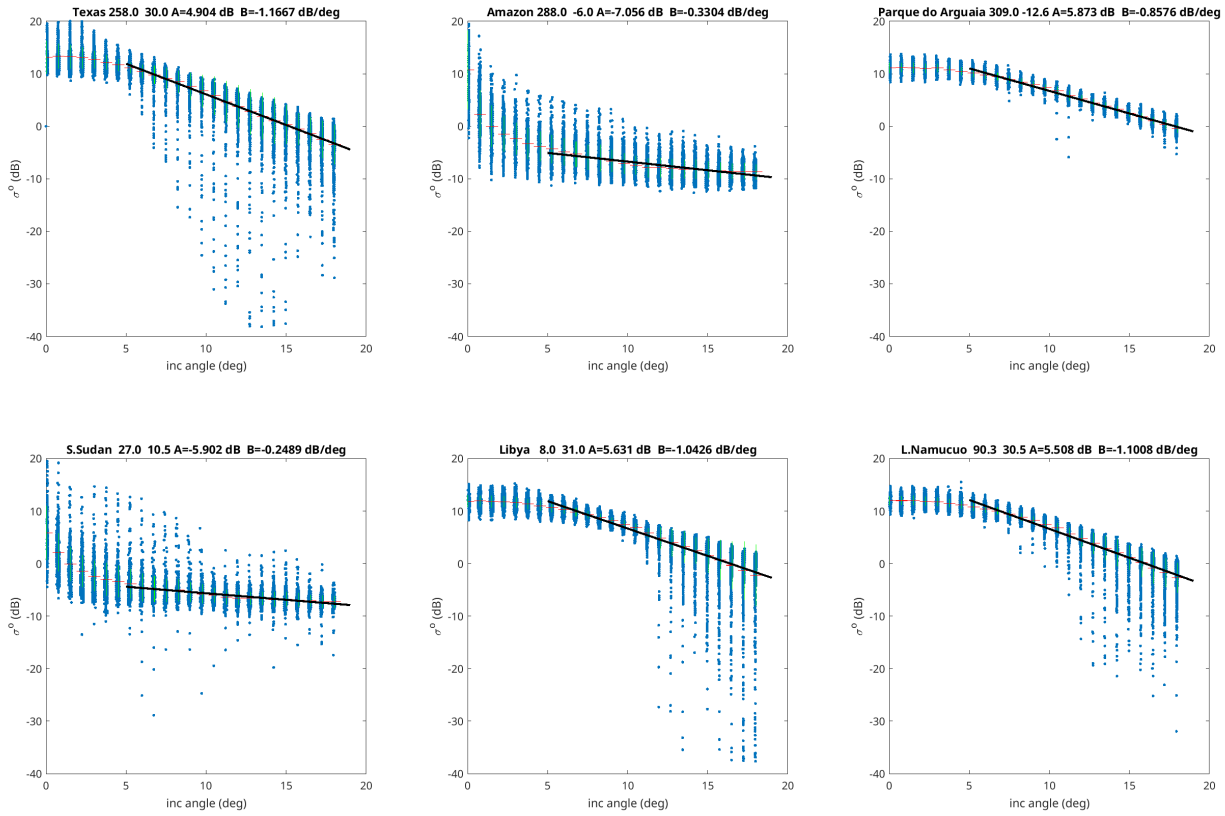

Figure 10: *Plots of TRMM PR σ^o versus incidence angles over a 28-day period (DOY 1-28, 2000) for different areas of the globe. Each plot shows values over 2° longitude by 1° latitude box. See text.*

In contrast, when multiple overlapping measurements are available, i.e., the surface is oversampled, it is possible to obtain images with the finest effective resolution using the SIR imaging algorithm. While not as effective as full SIR, the AVE algorithm also provides improved resolution compared to simple gridding.

Enhancement of the effective resolution *requires* dense sampling of the surface. This is the reason multiple passes are used. In addition, multiple measurements at a diversity of incidence angles are required to estimate the incidence angle slope and the azimuth modulation. When the surface is adequately sampled, the effective spatial resolution is improved, which can result in a reduction in noise. However, when the surface is undersampled, it is difficult for the image resolution to be much better than the MRF resolution.

6.3 Data Volume

Table 5 summarizes available CETB *TRMM PR* radar products, which are all in CETB-standard EASE-2 Grid projections. In this table, "days" refers to the length of time used for image formation. Imaging periods overlap, with a new image started each day. Individual file sizes vary due to internal file compression for each type of image. See Section 4.5 for access details.

7 Acknowledgments

This work was conducted as part of the Brigham Young University Scatterometer Climate Record Pathfinder and was supported in part by NASA Grant #80NSSC19K0057.

8 References

References

Brodzik, M. J., B. Billingsley, T. Haran, B. Raup, and M. H. Savoie. 2012. EASE-Grid 2.0: Incremental but significant improvements for Earth-gridded data sets. *International Society for Photogrammetry and Remote Sensing 1*, 32–45. doi:10.3390/ijgi101003.

Brodzik, M. J., B. Billingsley, T. Haran, B. Raup, and M. H. Savoie. 2014. Correction: Brodzik, M.J., *et al.* EASE-Grid 2.0: Incremental but Significant Improvements for Earth-Gridded Data Sets, *ISPRS Int. J. Geo-Inf.* 2012, 1, 32–45. *ISPRS Int. J. Geo-Inf. 3*, 1154–1156. doi:10.3390/ijgi3031154.

Brodzik, M. J., D. G. Long, M. A. Hardman, A. Paget, and R. L. Armstrong. 2016, updated 2021. MEaSUREs Calibrated Enhanced-Resolution Passive Microwave Daily EASE-Grid 2.0 Brightness Temperature ESDR, Version 1. National Snow and Ice Data Center, Boulder, CO USA. Digital Media, http://nsidc.org/data/nsidc-0630, doi:https://doi.org/10.5067/MEASURES/CRYOSPHERE/NSIDC-0630.001.

Brodzik, M. J., J. M. Ramage, M. A. Hardman, D. G. Long, and R. L. Armstrong. 2018. Improving melt onset detection in mountainous regions from the new, enhanced-resolution passive microwave climate record. Poster presentation at EGU General Assembly, CR 2.1:10690, Vienna, Austria, 9–13 April.

Early, D. S. and D. G. Long. 2001. Image reconstruction and enhanced resolution imaging from irregular samples. *IEEE Transactions on Geoscience and Remote Sensing 39*(2), 291–302. doi:10.1109/36.905237.

Kawanishi, T., H. Kuroiwa, M. Kojima, K. Oikawa, T. Kozu, H. Kumagai, K. Okamoto, M. Okumura, H. Nakatsuka, and K. Nishikawa. 2000. Trmm precipitation radar. *Advances in Space Research 25*(5), 969–972. Remote Sensing and Applications: Earth, Atmosphere and Oceans, doi:https://doi.org/10.1016/S0273-1177(99)00932-1.

Kozu, T., T. Kawanishi, H. Kuroiwa, M. Kojima, K. Oikawa, H. Kumagai, K. Okamoto, M. Okumura, H. Nakatsuka, and K. Nishikawa. 2001. Development of precipitation radar onboard the tropical rainfall measuring mission (trmm) satellite. *IEEE Transactions on Geoscience and Remote Sensing 39*(1), 102–116. doi:10.1109/36.898669.

Lindsley, R., C. Anderson, J. F.-S. na, and D. Long. 2016. A parameterized ASCAT measurement spatial response function. *IEEE Transactions on Geoscience and Remote Sensing 54*(8), 4570–4579. doi:10.1109/TGRS.2016.2544835.

Long, D. and M. Brodzik. 2016a. Optimum image formation for spaceborne microwave radiometer products. *IEEE Trans. Geosci. Remote Sensing 54*(5), 2763–2779. doi:10.1109/TGARS.2015.2505677.

Long, D. and D. Daum. 1998. Spatial resolution enhancement of SSM/I data. *IEEE Trans. Geosci. Remote Sensing 36*(2), 407–417. doi:10.1109/36.662726.

Long, D. and R. Franz. 2016a. Band-limited signal reconstruction from irregular samples with variable apertures. *IEEE Transactions on Geoscience and Remote Sensing 54*(4), 2424–2436. doi:10.1109/TGRS.2015.2501366.

Long, D., P. Hardin, and P. Whiting. 1993. Resolution enhancement of spaceborne scatterometer data. *IEEE Trans. Geosci. Remote Sensing 31*(3), 700–715. doi:10.1109/36.225536.

Long, D. and J. Z. Miller. 2023. NSCAT twice-daily SIR-enhanced scatterometer EASE-grid 2.0 radar backscatter Algorithm Theoretical Basis Document. doi:https://doi.org/10.5281/zenodo.11199226.

Long, D. and J. Z. Miller. 2024. ASCAT twice-daily SIR-enhanced scatterometer EASE-grid 2.0 radar backscatter Algorithm Theoretical Basis Document. doi:https://doi.org/10.5281/zenodo.14582508.

Long, D. G.. 2017. Comparison of SeaWinds backscatter imaging algorithms. *IEEE J. Sel. Topics in Applied Earth Observations 10*(3), 2214–2231. doi:10.1109/JSTARS.2016.2626966.

Long, D. G. and M. J. Brodzik. 2016b, May. Optimum Image Formation for Spaceborne Microwave Radiometer Products. *IEEE Transactions on Geoscience and Remote Sensing 54*(5), 2763–2779. doi:10.1109/TGRS.2015.2505677.

Long, D. G., M. J. Brodzik, and M. A. Hardman. 2019. Enhanced–Resolution SMAP Brightness Temperature Image Products. *IEEE Transactions on Geoscience and Remote Sensing 57*(7), 4151–4163. doi:10.1109/TGRS.2018.2889427.

Long, D. G. and R. O. W. Franz. 2016b. Band–limited Signal Reconstruction from Irregular Samples with Variable Apertures. *IEEE Transactions on Geoscience and Remote Sensing 54*(4), 2424–2436. doi:10.1109/TGRS.2015.2501366.

Pitas, I. and A. Venetsanopoulos. 1986. Nonlinear mean filters in image processing. *IEEE Transactions on Acoustics, Speech, and Signal Processing 34*(3), 573–584. doi:10.1109/TASSP.1986.1164857.

Simpson, J., R. F. Adler, and G. R. North. 1988. A proposed tropical rainfall measuring mission (TRMM) satellite. *Bulletin of the American Meteorological Society 69*(3), 278–295. doi:https://doi.org/10.1175/1520-0477(1988)069<0278:APTRMM>2.0.CO;2.

Team, T. P. R.. 2011a. Tropical rainfall measuring mission (TRMM) precipitation radar algorithm – instruction manual for version 7.

Team, T. P. R.. 2011b. Tropical rainfall measuring mission (TRMM) precipitation radar algorithm – instruction manual for version 7.

Ulaby, F. T. and D. G. Long. 2014. *Microwave Radar and Radiometric Remote Sensing*. Ann Arbor, MI, USA: University of Michigan Press.

Wikipedia. visited 8 Oct. 2016. Geometric mean. Online, http://en.wikipedia.org/wiki/Geometric_mean.

Appendices

A *TRMM PR* Projections and Grids

Table 6: TRMM PR *25 km product EASE-Grid 2.0 projections and grid dimensions produced for compatibility with CETB ESDR data products (Brodzik et al., 2021)*.

Name	Projection	Resolution (km)	Cols	Rows	Latitude Extent	Longitude Extent
EASE2-T25km	Temperate and Tropical Cylindrical	25.02526000	1388	540	$\pm$67.0576406°	$\pm$180°

Note: While the CETB product definitions include polar regions, these are not produced for TRMM PR products since the TRMM PR does not provide coverage in these regions.

B *TRMM PR* Data Definition

B.1 File Requirements

Following Brodzik et al. (2021), *TRMM PR* product file requirements as implemented for the *TRMM PR* product include:

- File size maximum is less < 4 MB
- Files conform to netCDF-CF 1.6 conventions for all but the requirement that puts the lat/lon arrays into the file; however, CF-compliant coordinate variables with projected coordinate locations are included
- Files pass CF-compliance-checking for all but the lat/lon arrays using the JPL compliance-checker
- Each file contains 1 or more array variables, with associated ancillary variables, possibly different ancillary variables for each gridding technique
- Each file of the same type (GRD or SIR) contains the same file-level metadata for that type
- Time values are machine- and human-readable
- Projection metadata may be in multiple forms (a proj4 string and/or a WKT string)
- Variable/attribute names CF-compliant whenever possible

The *TRMM PR* .nc files work with gdal utility, *gdal_translate*, to produce a geoTIFF version of each of the data variables <variable_name> in the file, (details in Brodzik et al. (2018)), for e.g.:

```
$ gdal_translate -of GTiff -b 1 \
NETCDF:''cetb.nc'':<variable_name> variable_name.tif
```

B.2 Filename Convention

TRMM PR data are distributed by the NSIDC DAAC (`https://doi.org/10.5067/WK4DZ1LG4L6O`). Filenames are:
<product-id>_<platform-sensor>_<algorithm>_<grid-name>_<pass>_<channel>
<yyyymmdd>-<yyyymmdd><version>.nc
where parts of the filename are described in Table 7.

B.3 File Content, v1.0

The following is a sample NetCDF *ncdump –h* utility output for a particular *TRMM PR* v1.0 25 km AVE product file. File-level metadata and processing details vary depending on projection, spatial resolution and processing details (method, input file list, etc.).

Table 7: TRMM PR *filenaming convention*

Part	Description	Values
<product_id>	NSIDC unique data product id	NSIDC-0807
<platform>	Satellite platform	TRMM
<sensor>	Sensor name	PR
<algorithm>	Reconstruction algorithm	GRD
<grid_name>	EASE-Grid 2.0 grid id	T25km
<pass>	Pass direction (T grids)	T
<channel>	Channel (frequency in GHz and polarization)	13.4HH
<yyyymmdd>	Date	4-digit year, 2-digit month, and 2-digit day-of-month start
<yyyymmdd>	Date	4-digit year, 2-digit month, and 2-digit day-of-month stop
<version>	Version number	production version number

```
netcdf NSIDC-0807_TRMM-PR_GRD_EASE2_T25KM_B_13.4HH_20130326-20130422_V1.0 {
dimensions:
 time = UNLIMITED ; // (1 currently)
 y = 540 ;
 x = 1388 ;
variables:
 double time(time) ;
  time:standard_name = "time" ;
  time:coverage_content_type = "coordinate" ;
  time:long_name = "ANSI date" ;
  time:units = "days since 1972-01-01 00:00:00" ;
  time:calendar = "gregorian" ;
  time:axis = "T" ;
  time:valid_range = 0., 1.79769313486232e+308 ;
 double y(y) ;
  y:standard_name = "projection_y_coordinate" ;
  y:coverage_content_type = "coordinate" ;
  y:long_name = "y" ;
  y:units = "meters" ;
  y:axis = "Y" ;
  y:valid_range = -6756820.2, 6756820.2 ;
 double x(x) ;
  x:standard_name = "projection_x_coordinate" ;
```

```
  x:coverage_content_type = "coordinate" ;
  x:long_name = "x" ;
  x:units = "meters" ;
  x:axis = "X" ;
  x:valid_range = -17367530.44, 17367530.44 ;
 char crs ;
  crs:grid_mapping_name = "lambert_cylindrical_equal_area" ;
  crs:longitude_of_central_meridian = 0. ;
  crs:standard_parallel = 30. ;
  crs:false_easting = 0. ;
  crs:false_northing = 0. ;
  crs:semi_major_axis = 6378137. ;
  crs:inverse_flattening = 298.257223563 ;
  crs:proj4text = "+proj=cea +lat_0=0 +lon_0=0 +lat_ts=30 +x_0=0 +y_0=0 +ellps=WGS84 +da
  crs:srid = "urn:ogc:def:crs:EPSG::6933" ;
  crs:coverage_content_type = "auxiliaryInformation" ;
  crs:references = "[\"EASE-Grid 2.0 documentation: http://nsidc.org/data/ease/ease_grid
  crs:crs_wkt = "PROJCRS[\"WGS 84 / NSIDC EASE-Grid 2.0 Global\", BASEGEODCRS[\"WGS 84\"
  crs:long_name = "EASE2_T25km" ;
 short Sigma0(time, y, x) ;
  Sigma0:standard_name = "normalized_radar_cross_section" ;
  Sigma0:long_name = "GRD Sigma0" ;
  Sigma0:units = "1" ;
  Sigma0:comment_on_units = "unitless, stored as dB=10*log10()" ;
  Sigma0:_FillValue = -32768s ;
  Sigma0:valid_range = 0s, 32767s ;
  Sigma0:packing_convention = "netCDF" ;
  Sigma0:packing_convention_description = "unpacked = scale_factor*packed + add_offset"
  Sigma0:scale_factor = 0.002f ;
  Sigma0:add_offset = -55.f ;
  Sigma0:grid_mapping = "crs" ;
  Sigma0:coverage_content_type = "image" ;
  Sigma0:median_filter = 0 ;
 short Sigma0_slope(time, y, x) ;
  Sigma0_slope:standard_name = "derivative_of_normalized_radar_cross_section_wrt_angle_o
  Sigma0_slope:long_name = "GRD Sigma0 slope" ;
  Sigma0_slope:units = "1" ;
  Sigma0_slope:comment_on_units = "dB/deg, dB=10*log10()" ;
  Sigma0_slope:_FillValue = -32768s ;
  Sigma0_slope:valid_range = 0s, 32767s ;
```

```
 Sigma0_slope:packing_convention = "netCDF" ;
 Sigma0_slope:packing_convention_description = "unpacked = scale_factor*packed + add_of
 Sigma0_slope:scale_factor = 0.001f ;
 Sigma0_slope:add_offset = -2.f ;
 Sigma0_slope:grid_mapping = "crs" ;
 Sigma0_slope:coverage_content_type = "image" ;
short Sigma0_num_samples(time, y, x) ;
 Sigma0_num_samples:long_name = "GRD Number of Measurements" ;
 Sigma0_num_samples:units = "count" ;
 Sigma0_num_samples:_FillValue = 0s ;
 Sigma0_num_samples:valid_range = 1s, 255s ;
 Sigma0_num_samples:grid_mapping = "crs" ;
 Sigma0_num_samples:coverage_content_type = "auxiliaryInformation" ;
short Sigma0_std_dev(time, y, x) ;
 Sigma0_std_dev:long_name = "GRD Sigma0 standard deviation" ;
 Sigma0_std_dev:units = "1" ;
 Sigma0_std_dev:comment_on_units = "unitless, stored as dB=10*log10()" ;
 Sigma0_std_dev:_FillValue = -32768s ;
 Sigma0_std_dev:valid_range = 0s, 32767s ;
 Sigma0_std_dev:packing_convention = "netCDF" ;
 Sigma0_std_dev:packing_convention_description = "unpacked = scale_factor*packed + add_
 Sigma0_std_dev:scale_factor = 0.002f ;
 Sigma0_std_dev:add_offset = 0.f ;
 Sigma0_std_dev:grid_mapping = "crs" ;
 Sigma0_std_dev:coverage_content_type = "auxiliaryInformation" ;
short Incidence_angle(time, y, x) ;
 Incidence_angle:long_name = "GRD Incidence Angle" ;
 Incidence_angle:units = "degree" ;
 Incidence_angle:_FillValue = -1s ;
 Incidence_angle:valid_range = 0s, 9000s ;
 Incidence_angle:packing_convention = "netCDF" ;
 Incidence_angle:packing_convention_description = "unpacked = scale_factor*packed + add
 Incidence_angle:scale_factor = 0.01f ;
 Incidence_angle:add_offset = 0.f ;
 Incidence_angle:grid_mapping = "crs" ;
 Incidence_angle:coverage_content_type = "auxiliaryInformation" ;
short Sigma0_time(time, y, x) ;
 Sigma0_time:long_name = "Time of Day" ;
 Sigma0_time:units = "minutes since 2013-03-26 00:00:00" ;
 Sigma0_time:_FillValue = -32768s ;
```

```
  Sigma0_time:valid_range = -32767s, 32767s ;
  Sigma0_time:packing_convention = "netCDF" ;
  Sigma0_time:packing_convention_description = "unpacked = scale_factor*packed + add_off
  Sigma0_time:scale_factor = 1.f ;
  Sigma0_time:add_offset = 0.f ;
  Sigma0_time:grid_mapping = "crs" ;
  Sigma0_time:coverage_content_type = "auxiliaryInformation" ;
  Sigma0_time:calendar = "gregorian" ;

// global attributes:
  :references = "Early, D. S., and D.G. Long. 2001. Image Reconstruction and Enhanced Re
  :title = "TRMM Precipitation Radar SIR-Enhanced EASE-Grid 2.0 Surface Radar Backscatte
  :id = "doi:10.5067/WK4DZ1LG4L60" ;
  :summary = "Enhanced-resolution, gridded TRMMPR Ku-band radar backscatter" ;
  :project = "Scatterometer Climate Record Pathfinder" ;
  :contributor_name = "David G. Long, NASA Scatterometer Climate Record Pathfinder" ;
  :contributor_role = "Principal Investigator and Developer, Data Producer" ;
  :citation = "Long, D.G., and J.Z. Miller, 2025. TRMM Precipitation Radar SIR-Enhanced
  :license = "These data are freely, openly, and fully available to use without\nrestric
  :Conventions = "CF-1.6, ACDD-1.3" ;
  :product_version = "v1.0" ;
  :software_version_id = "BYU03.00" ;
  :software_repository = "" ;
  :history = "trmmpr_sir_cetb" ;
  :comment = "Epoch date for data in this file: 2013-03-26 00:00:00Z" ;
  :source = ": See input_fileN list and number_of_input_files attributes" ;
  :metadata_link = "http://www.scp.byu.edu/" ;
  :institution = "Scatterometer Climate Record Pathfinder\nElectrical and Computer Engin
  :publisher_name = "Scatterometer Climate Record Pathfinder" ;
  :publisher_type = "institution" ;
  :publisher_url = "http://www.scp.byu.edu" ;
  :publisher_email = "long@ee.byu.edu" ;
  :program = "NASA Earth Science Data and Information System (ESDIS)" ;
  :standard_name_vocabulary = "CF Standard Name Table (v27, 28 September 2013)" ;
  :cdm_data_type = "Grid" ;
  :keywords = "EARTH SCIENCE > SPECTRAL/ENGINEERING > MICROWAVE > RADAR BACKSCATTER" ;
  :keywords_vocabulary = "NASA Global Change Master Directory (GCMD) Earth Science Keywo
  :platform = "TRMM > TRMM Precipitation Radar" ;
  :platform_vocabulary = "TRMM > TRMM Precipitation Radar" ;
  :instrument = "TRMM-PR Ku-BAND RADAR > TRMM-PR Ku-Band Radar" ;
```

```
:instrument_vocabulary = "NASA Global Change Master Directory (GCMD) Earth Science Key
:time_coverage_resolution = "P1d" ;
:geospatial_lat_min = -67.057541 ;
:geospatial_lat_max = 67.057541 ;
:geospatial_lon_min = -180. ;
:geospatial_lon_max = 180. ;
:geospatial_x_units = "meters" ;
:geospatial_y_units = "meters" ;
:naming_authority = "org.doi.dx" ;
:date_created = "2024-12-15T22:13:17GMT" ;
:date_modified = "2024-12-15T22:13:17GMT" ;
:date_issued = "2024-12-15T22:13:17GMT" ;
:date_metadata_modified = "2024-12-15T22:13:17GMT" ;
:input_data_quality_filtering = "Only used highest-quality input data." ;
:acknowledgement = "This data set was created with funding from NASA Grant #TBD." ;
:processing_level = "Level 3" ;
:creator_name = "David Long" ;
:creator_type = "person" ;
:creator_email = "long@ee.byu.edu" ;
:creator_url = "http://www.scp.byu.edu" ;
:creator_institution = "Electrical and Computer Engineering Department\nBrigham Young
:geospatial_bounds = "POLYGON((-67.057541 -180.000000, -67.057541 180.000000, 67.05754
:geospatial_bounds_crs = "EPSG:6933" ;
:geospatial_lat_units = "degrees_north" ;
:geospatial_lon_units = "degrees_east" ;
:geospatial_x_resolution = "25025.26 meters" ;
:geospatial_y_resolution = "25025.26 meters" ;
:time_coverage_start = "2013-03-27T08:02:00.00Z" ;
:time_coverage_end = "2013-04-19T19:34:00.00Z" ;
:time_coverage_duration = "P23T11:32:00.00" ;
:number_of_input_files = 436 ;
:input_file1 = "2A21.20130326.87487.7.h5" ;
:input_file2 = "2A21.20130326.87488.7.h5" ;
:input_file3 = "2A21.20130326.87489.7.h5" ;
:input_file4 = "2A21.20130326.87490.7.h5" ;
:input_file5 = "2A21.20130326.87491.7.h5" ;
:input_file6 = "2A21.20130326.87492.7.h5" ;
:input_file7 = "2A21.20130326.87493.7.h5" ;
:input_file8 = "2A21.20130326.87494.7.h5" ;
:input_file9 = "2A21.20130326.87495.7.h5" ;
```

```
:input_file10 = "2A21.20130326.87496.7.h5" ;
:input_file11 = "2A21.20130326.87497.7.h5" ;
:input_file12 = "2A21.20130326.87498.7.h5" ;
:input_file13 = "2A21.20130326.87499.7.h5" ;
:input_file14 = "2A21.20130326.87500.7.h5" ;
:input_file15 = "2A21.20130327.87501.7.h5" ;
:input_file16 = "2A21.20130327.87502.7.h5" ;
:input_file17 = "2A21.20130327.87503.7.h5" ;
:input_file18 = "2A21.20130327.87504.7.h5" ;
:input_file19 = "2A21.20130327.87505.7.h5" ;
:input_file20 = "2A21.20130327.87506.7.h5" ;
:input_file21 = "2A21.20130327.87507.7.h5" ;
:input_file22 = "2A21.20130327.87508.7.h5" ;
:input_file23 = "2A21.20130327.87509.7.h5" ;
:input_file24 = "2A21.20130327.87510.7.h5" ;
:input_file25 = "2A21.20130327.87511.7.h5" ;
:input_file26 = "2A21.20130327.87512.7.h5" ;
:input_file27 = "2A21.20130327.87513.7.h5" ;
:input_file28 = "2A21.20130327.87514.7.h5" ;
:input_file29 = "2A21.20130327.87515.7.h5" ;
:input_file30 = "2A21.20130327.87516.7.h5" ;
:input_file31 = "2A21.20130328.87517.7.h5" ;
:input_file32 = "2A21.20130328.87518.7.h5" ;
:input_file33 = "2A21.20130328.87519.7.h5" ;
:input_file34 = "2A21.20130328.87520.7.h5" ;
:input_file35 = "2A21.20130328.87521.7.h5" ;
:input_file36 = "2A21.20130328.87522.7.h5" ;
:input_file37 = "2A21.20130328.87523.7.h5" ;
:input_file38 = "2A21.20130328.87524.7.h5" ;
:input_file39 = "2A21.20130328.87525.7.h5" ;
:input_file40 = "2A21.20130328.87526.7.h5" ;
:input_file41 = "2A21.20130328.87527.7.h5" ;
:input_file42 = "2A21.20130328.87528.7.h5" ;
:input_file43 = "2A21.20130328.87529.7.h5" ;
:input_file44 = "2A21.20130328.87530.7.h5" ;
:input_file45 = "2A21.20130328.87531.7.h5" ;
:input_file46 = "2A21.20130329.87532.7.h5" ;
:input_file47 = "2A21.20130329.87533.7.h5" ;
:input_file48 = "2A21.20130329.87534.7.h5" ;
:input_file49 = "2A21.20130329.87535.7.h5" ;
```

```
:input_file50 = "2A21.20130329.87536.7.h5" ;
:input_file51 = "2A21.20130329.87537.7.h5" ;
:input_file52 = "2A21.20130329.87538.7.h5" ;
:input_file53 = "2A21.20130329.87539.7.h5" ;
:input_file54 = "2A21.20130329.87540.7.h5" ;
:input_file55 = "2A21.20130329.87541.7.h5" ;
:input_file56 = "2A21.20130329.87542.7.h5" ;
:input_file57 = "2A21.20130329.87543.7.h5" ;
:input_file58 = "2A21.20130329.87544.7.h5" ;
:input_file59 = "2A21.20130329.87545.7.h5" ;
:input_file60 = "2A21.20130329.87546.7.h5" ;
:input_file61 = "2A21.20130329.87547.7.h5" ;
:input_file62 = "2A21.20130330.87548.7.h5" ;
:input_file63 = "2A21.20130330.87549.7.h5" ;
:input_file64 = "2A21.20130330.87550.7.h5" ;
:input_file65 = "2A21.20130330.87551.7.h5" ;
:input_file66 = "2A21.20130330.87552.7.h5" ;
:input_file67 = "2A21.20130330.87553.7.h5" ;
:input_file68 = "2A21.20130330.87554.7.h5" ;
:input_file69 = "2A21.20130330.87555.7.h5" ;
:input_file70 = "2A21.20130330.87556.7.h5" ;
:input_file71 = "2A21.20130330.87557.7.h5" ;
:input_file72 = "2A21.20130330.87558.7.h5" ;
:input_file73 = "2A21.20130330.87559.7.h5" ;
:input_file74 = "2A21.20130330.87560.7.h5" ;
:input_file75 = "2A21.20130330.87561.7.h5" ;
:input_file76 = "2A21.20130330.87562.7.h5" ;
:input_file77 = "2A21.20130331.87563.7.h5" ;
:input_file78 = "2A21.20130331.87564.7.h5" ;
:input_file79 = "2A21.20130331.87565.7.h5" ;
:input_file80 = "2A21.20130331.87566.7.h5" ;
:input_file81 = "2A21.20130331.87567.7.h5" ;
:input_file82 = "2A21.20130331.87568.7.h5" ;
:input_file83 = "2A21.20130331.87569.7.h5" ;
:input_file84 = "2A21.20130331.87570.7.h5" ;
:input_file85 = "2A21.20130331.87571.7.h5" ;
:input_file86 = "2A21.20130331.87572.7.h5" ;
:input_file87 = "2A21.20130331.87573.7.h5" ;
:input_file88 = "2A21.20130331.87574.7.h5" ;
:input_file89 = "2A21.20130331.87575.7.h5" ;
```

```
:input_file90 = "2A21.20130331.87576.7.h5" ;
:input_file91 = "2A21.20130331.87577.7.h5" ;
:input_file92 = "2A21.20130331.87578.7.h5" ;
:input_file93 = "2A21.20130401.87579.7.h5" ;
:input_file94 = "2A21.20130401.87580.7.h5" ;
:input_file95 = "2A21.20130401.87581.7.h5" ;
:input_file96 = "2A21.20130401.87582.7.h5" ;
:input_file97 = "2A21.20130401.87583.7.h5" ;
:input_file98 = "2A21.20130401.87584.7.h5" ;
:input_file99 = "2A21.20130401.87585.7.h5" ;
:input_file100 = "2A21.20130401.87586.7.h5" ;
:input_file101 = "2A21.20130401.87587.7.h5" ;
:input_file102 = "2A21.20130401.87588.7.h5" ;
:input_file103 = "2A21.20130401.87589.7.h5" ;
:input_file104 = "2A21.20130401.87590.7.h5" ;
:input_file105 = "2A21.20130401.87591.7.h5" ;
:input_file106 = "2A21.20130401.87592.7.h5" ;
:input_file107 = "2A21.20130401.87593.7.h5" ;
:input_file108 = "2A21.20130401.87594.7.h5" ;
:input_file109 = "2A21.20130402.87595.7.h5" ;
:input_file110 = "2A21.20130402.87596.7.h5" ;
:input_file111 = "2A21.20130402.87597.7.h5" ;
:input_file112 = "2A21.20130402.87598.7.h5" ;
:input_file113 = "2A21.20130402.87599.7.h5" ;
:input_file114 = "2A21.20130402.87600.7.h5" ;
:input_file115 = "2A21.20130402.87601.7.h5" ;
:input_file116 = "2A21.20130402.87602.7.h5" ;
:input_file117 = "2A21.20130402.87603.7.h5" ;
:input_file118 = "2A21.20130402.87604.7.h5" ;
:input_file119 = "2A21.20130402.87605.7.h5" ;
:input_file120 = "2A21.20130402.87606.7.h5" ;
:input_file121 = "2A21.20130402.87607.7.h5" ;
:input_file122 = "2A21.20130402.87608.7.h5" ;
:input_file123 = "2A21.20130402.87609.7.h5" ;
:input_file124 = "2A21.20130403.87610.7.h5" ;
:input_file125 = "2A21.20130403.87611.7.h5" ;
:input_file126 = "2A21.20130403.87612.7.h5" ;
:input_file127 = "2A21.20130403.87613.7.h5" ;
:input_file128 = "2A21.20130403.87614.7.h5" ;
:input_file129 = "2A21.20130403.87615.7.h5" ;
```

```
:input_file130 = "2A21.20130403.87616.7.h5" ;
:input_file131 = "2A21.20130403.87617.7.h5" ;
:input_file132 = "2A21.20130403.87618.7.h5" ;
:input_file133 = "2A21.20130403.87619.7.h5" ;
:input_file134 = "2A21.20130403.87620.7.h5" ;
:input_file135 = "2A21.20130403.87621.7.h5" ;
:input_file136 = "2A21.20130403.87622.7.h5" ;
:input_file137 = "2A21.20130403.87623.7.h5" ;
:input_file138 = "2A21.20130403.87624.7.h5" ;
:input_file139 = "2A21.20130403.87625.7.h5" ;
:input_file140 = "2A21.20130404.87626.7.h5" ;
:input_file141 = "2A21.20130404.87627.7.h5" ;
:input_file142 = "2A21.20130404.87628.7.h5" ;
:input_file143 = "2A21.20130404.87629.7.h5" ;
:input_file144 = "2A21.20130404.87630.7.h5" ;
:input_file145 = "2A21.20130404.87631.7.h5" ;
:input_file146 = "2A21.20130404.87632.7.h5" ;
:input_file147 = "2A21.20130404.87633.7.h5" ;
:input_file148 = "2A21.20130404.87634.7.h5" ;
:input_file149 = "2A21.20130404.87635.7.h5" ;
:input_file150 = "2A21.20130404.87636.7.h5" ;
:input_file151 = "2A21.20130404.87637.7.h5" ;
:input_file152 = "2A21.20130404.87638.7.h5" ;
:input_file153 = "2A21.20130404.87639.7.h5" ;
:input_file154 = "2A21.20130404.87640.7.h5" ;
:input_file155 = "2A21.20130405.87641.7.h5" ;
:input_file156 = "2A21.20130405.87642.7.h5" ;
:input_file157 = "2A21.20130405.87643.7.h5" ;
:input_file158 = "2A21.20130405.87644.7.h5" ;
:input_file159 = "2A21.20130405.87645.7.h5" ;
:input_file160 = "2A21.20130405.87646.7.h5" ;
:input_file161 = "2A21.20130405.87647.7.h5" ;
:input_file162 = "2A21.20130405.87648.7.h5" ;
:input_file163 = "2A21.20130405.87649.7.h5" ;
:input_file164 = "2A21.20130405.87650.7.h5" ;
:input_file165 = "2A21.20130405.87651.7.h5" ;
:input_file166 = "2A21.20130405.87652.7.h5" ;
:input_file167 = "2A21.20130405.87653.7.h5" ;
:input_file168 = "2A21.20130405.87654.7.h5" ;
:input_file169 = "2A21.20130405.87655.7.h5" ;
```

```
:input_file170 = "2A21.20130405.87656.7.h5" ;
:input_file171 = "2A21.20130406.87657.7.h5" ;
:input_file172 = "2A21.20130406.87658.7.h5" ;
:input_file173 = "2A21.20130406.87659.7.h5" ;
:input_file174 = "2A21.20130406.87660.7.h5" ;
:input_file175 = "2A21.20130406.87661.7.h5" ;
:input_file176 = "2A21.20130406.87662.7.h5" ;
:input_file177 = "2A21.20130406.87663.7.h5" ;
:input_file178 = "2A21.20130406.87664.7.h5" ;
:input_file179 = "2A21.20130406.87665.7.h5" ;
:input_file180 = "2A21.20130406.87666.7.h5" ;
:input_file181 = "2A21.20130406.87667.7.h5" ;
:input_file182 = "2A21.20130406.87668.7.h5" ;
:input_file183 = "2A21.20130406.87669.7.h5" ;
:input_file184 = "2A21.20130406.87670.7.h5" ;
:input_file185 = "2A21.20130406.87671.7.h5" ;
:input_file186 = "2A21.20130406.87672.7.h5" ;
:input_file187 = "2A21.20130407.87673.7.h5" ;
:input_file188 = "2A21.20130407.87674.7.h5" ;
:input_file189 = "2A21.20130407.87675.7.h5" ;
:input_file190 = "2A21.20130407.87676.7.h5" ;
:input_file191 = "2A21.20130407.87677.7.h5" ;
:input_file192 = "2A21.20130407.87678.7.h5" ;
:input_file193 = "2A21.20130407.87679.7.h5" ;
:input_file194 = "2A21.20130407.87680.7.h5" ;
:input_file195 = "2A21.20130407.87681.7.h5" ;
:input_file196 = "2A21.20130407.87682.7.h5" ;
:input_file197 = "2A21.20130407.87683.7.h5" ;
:input_file198 = "2A21.20130407.87684.7.h5" ;
:input_file199 = "2A21.20130407.87685.7.h5" ;
:input_file200 = "2A21.20130407.87686.7.h5" ;
:input_file201 = "2A21.20130407.87687.7.h5" ;
:input_file202 = "2A21.20130408.87688.7.h5" ;
:input_file203 = "2A21.20130408.87689.7.h5" ;
:input_file204 = "2A21.20130408.87690.7.h5" ;
:input_file205 = "2A21.20130408.87691.7.h5" ;
:input_file206 = "2A21.20130408.87692.7.h5" ;
:input_file207 = "2A21.20130408.87693.7.h5" ;
:input_file208 = "2A21.20130408.87694.7.h5" ;
:input_file209 = "2A21.20130408.87695.7.h5" ;
```

```
:input_file210 = "2A21.20130408.87696.7.h5" ;
:input_file211 = "2A21.20130408.87697.7.h5" ;
:input_file212 = "2A21.20130408.87698.7.h5" ;
:input_file213 = "2A21.20130408.87699.7.h5" ;
:input_file214 = "2A21.20130408.87700.7.h5" ;
:input_file215 = "2A21.20130408.87701.7.h5" ;
:input_file216 = "2A21.20130408.87702.7.h5" ;
:input_file217 = "2A21.20130408.87703.7.h5" ;
:input_file218 = "2A21.20130409.87704.7.h5" ;
:input_file219 = "2A21.20130409.87705.7.h5" ;
:input_file220 = "2A21.20130409.87706.7.h5" ;
:input_file221 = "2A21.20130409.87707.7.h5" ;
:input_file222 = "2A21.20130409.87708.7.h5" ;
:input_file223 = "2A21.20130409.87709.7.h5" ;
:input_file224 = "2A21.20130409.87710.7.h5" ;
:input_file225 = "2A21.20130409.87711.7.h5" ;
:input_file226 = "2A21.20130409.87712.7.h5" ;
:input_file227 = "2A21.20130409.87713.7.h5" ;
:input_file228 = "2A21.20130409.87714.7.h5" ;
:input_file229 = "2A21.20130409.87715.7.h5" ;
:input_file230 = "2A21.20130409.87716.7.h5" ;
:input_file231 = "2A21.20130409.87717.7.h5" ;
:input_file232 = "2A21.20130409.87718.7.h5" ;
:input_file233 = "2A21.20130410.87719.7.h5" ;
:input_file234 = "2A21.20130410.87720.7.h5" ;
:input_file235 = "2A21.20130410.87721.7.h5" ;
:input_file236 = "2A21.20130410.87722.7.h5" ;
:input_file237 = "2A21.20130410.87723.7.h5" ;
:input_file238 = "2A21.20130410.87724.7.h5" ;
:input_file239 = "2A21.20130410.87725.7.h5" ;
:input_file240 = "2A21.20130410.87726.7.h5" ;
:input_file241 = "2A21.20130410.87727.7.h5" ;
:input_file242 = "2A21.20130410.87728.7.h5" ;
:input_file243 = "2A21.20130410.87729.7.h5" ;
:input_file244 = "2A21.20130410.87730.7.h5" ;
:input_file245 = "2A21.20130410.87731.7.h5" ;
:input_file246 = "2A21.20130410.87732.7.h5" ;
:input_file247 = "2A21.20130410.87733.7.h5" ;
:input_file248 = "2A21.20130410.87734.7.h5" ;
:input_file249 = "2A21.20130411.87735.7.h5" ;
```

```
:input_file250 = "2A21.20130411.87736.7.h5" ;
:input_file251 = "2A21.20130411.87737.7.h5" ;
:input_file252 = "2A21.20130411.87738.7.h5" ;
:input_file253 = "2A21.20130411.87739.7.h5" ;
:input_file254 = "2A21.20130411.87740.7.h5" ;
:input_file255 = "2A21.20130411.87741.7.h5" ;
:input_file256 = "2A21.20130411.87742.7.h5" ;
:input_file257 = "2A21.20130411.87743.7.h5" ;
:input_file258 = "2A21.20130411.87744.7.h5" ;
:input_file259 = "2A21.20130411.87745.7.h5" ;
:input_file260 = "2A21.20130411.87746.7.h5" ;
:input_file261 = "2A21.20130411.87747.7.h5" ;
:input_file262 = "2A21.20130411.87748.7.h5" ;
:input_file263 = "2A21.20130411.87749.7.h5" ;
:input_file264 = "2A21.20130411.87750.7.h5" ;
:input_file265 = "2A21.20130412.87751.7.h5" ;
:input_file266 = "2A21.20130412.87752.7.h5" ;
:input_file267 = "2A21.20130412.87753.7.h5" ;
:input_file268 = "2A21.20130412.87754.7.h5" ;
:input_file269 = "2A21.20130412.87755.7.h5" ;
:input_file270 = "2A21.20130412.87756.7.h5" ;
:input_file271 = "2A21.20130412.87757.7.h5" ;
:input_file272 = "2A21.20130412.87758.7.h5" ;
:input_file273 = "2A21.20130412.87759.7.h5" ;
:input_file274 = "2A21.20130412.87760.7.h5" ;
:input_file275 = "2A21.20130412.87761.7.h5" ;
:input_file276 = "2A21.20130412.87762.7.h5" ;
:input_file277 = "2A21.20130412.87763.7.h5" ;
:input_file278 = "2A21.20130412.87764.7.h5" ;
:input_file279 = "2A21.20130412.87765.7.h5" ;
:input_file280 = "2A21.20130413.87766.7.h5" ;
:input_file281 = "2A21.20130413.87767.7.h5" ;
:input_file282 = "2A21.20130413.87768.7.h5" ;
:input_file283 = "2A21.20130413.87769.7.h5" ;
:input_file284 = "2A21.20130413.87770.7.h5" ;
:input_file285 = "2A21.20130413.87771.7.h5" ;
:input_file286 = "2A21.20130413.87772.7.h5" ;
:input_file287 = "2A21.20130413.87773.7.h5" ;
:input_file288 = "2A21.20130413.87774.7.h5" ;
:input_file289 = "2A21.20130413.87775.7.h5" ;
```

```
:input_file290 = "2A21.20130413.87776.7.h5" ;
:input_file291 = "2A21.20130413.87777.7.h5" ;
:input_file292 = "2A21.20130413.87778.7.h5" ;
:input_file293 = "2A21.20130413.87779.7.h5" ;
:input_file294 = "2A21.20130413.87780.7.h5" ;
:input_file295 = "2A21.20130413.87781.7.h5" ;
:input_file296 = "2A21.20130414.87782.7.h5" ;
:input_file297 = "2A21.20130414.87783.7.h5" ;
:input_file298 = "2A21.20130414.87784.7.h5" ;
:input_file299 = "2A21.20130414.87785.7.h5" ;
:input_file300 = "2A21.20130414.87786.7.h5" ;
:input_file301 = "2A21.20130414.87787.7.h5" ;
:input_file302 = "2A21.20130414.87788.7.h5" ;
:input_file303 = "2A21.20130414.87789.7.h5" ;
:input_file304 = "2A21.20130414.87790.7.h5" ;
:input_file305 = "2A21.20130414.87791.7.h5" ;
:input_file306 = "2A21.20130414.87792.7.h5" ;
:input_file307 = "2A21.20130414.87793.7.h5" ;
:input_file308 = "2A21.20130414.87794.7.h5" ;
:input_file309 = "2A21.20130414.87795.7.h5" ;
:input_file310 = "2A21.20130414.87796.7.h5" ;
:input_file311 = "2A21.20130415.87797.7.h5" ;
:input_file312 = "2A21.20130415.87798.7.h5" ;
:input_file313 = "2A21.20130415.87799.7.h5" ;
:input_file314 = "2A21.20130415.87800.7.h5" ;
:input_file315 = "2A21.20130415.87801.7.h5" ;
:input_file316 = "2A21.20130415.87802.7.h5" ;
:input_file317 = "2A21.20130415.87803.7.h5" ;
:input_file318 = "2A21.20130415.87804.7.h5" ;
:input_file319 = "2A21.20130415.87805.7.h5" ;
:input_file320 = "2A21.20130415.87806.7.h5" ;
:input_file321 = "2A21.20130415.87807.7.h5" ;
:input_file322 = "2A21.20130415.87808.7.h5" ;
:input_file323 = "2A21.20130415.87809.7.h5" ;
:input_file324 = "2A21.20130415.87810.7.h5" ;
:input_file325 = "2A21.20130415.87811.7.h5" ;
:input_file326 = "2A21.20130415.87812.7.h5" ;
:input_file327 = "2A21.20130416.87813.7.h5" ;
:input_file328 = "2A21.20130416.87814.7.h5" ;
:input_file329 = "2A21.20130416.87815.7.h5" ;
```

```
:input_file330 = "2A21.20130416.87816.7.h5" ;
:input_file331 = "2A21.20130416.87817.7.h5" ;
:input_file332 = "2A21.20130416.87818.7.h5" ;
:input_file333 = "2A21.20130416.87819.7.h5" ;
:input_file334 = "2A21.20130416.87820.7.h5" ;
:input_file335 = "2A21.20130416.87821.7.h5" ;
:input_file336 = "2A21.20130416.87822.7.h5" ;
:input_file337 = "2A21.20130416.87823.7.h5" ;
:input_file338 = "2A21.20130416.87824.7.h5" ;
:input_file339 = "2A21.20130416.87825.7.h5" ;
:input_file340 = "2A21.20130416.87826.7.h5" ;
:input_file341 = "2A21.20130416.87827.7.h5" ;
:input_file342 = "2A21.20130417.87828.7.h5" ;
:input_file343 = "2A21.20130417.87829.7.h5" ;
:input_file344 = "2A21.20130417.87830.7.h5" ;
:input_file345 = "2A21.20130417.87831.7.h5" ;
:input_file346 = "2A21.20130417.87832.7.h5" ;
:input_file347 = "2A21.20130417.87833.7.h5" ;
:input_file348 = "2A21.20130417.87834.7.h5" ;
:input_file349 = "2A21.20130417.87835.7.h5" ;
:input_file350 = "2A21.20130417.87836.7.h5" ;
:input_file351 = "2A21.20130417.87837.7.h5" ;
:input_file352 = "2A21.20130417.87838.7.h5" ;
:input_file353 = "2A21.20130417.87839.7.h5" ;
:input_file354 = "2A21.20130417.87840.7.h5" ;
:input_file355 = "2A21.20130417.87841.7.h5" ;
:input_file356 = "2A21.20130417.87842.7.h5" ;
:input_file357 = "2A21.20130417.87843.7.h5" ;
:input_file358 = "2A21.20130418.87844.7.h5" ;
:input_file359 = "2A21.20130418.87845.7.h5" ;
:input_file360 = "2A21.20130418.87846.7.h5" ;
:input_file361 = "2A21.20130418.87847.7.h5" ;
:input_file362 = "2A21.20130418.87848.7.h5" ;
:input_file363 = "2A21.20130418.87849.7.h5" ;
:input_file364 = "2A21.20130418.87850.7.h5" ;
:input_file365 = "2A21.20130418.87851.7.h5" ;
:input_file366 = "2A21.20130418.87852.7.h5" ;
:input_file367 = "2A21.20130418.87853.7.h5" ;
:input_file368 = "2A21.20130418.87854.7.h5" ;
:input_file369 = "2A21.20130418.87855.7.h5" ;
```

```
:input_file370 = "2A21.20130418.87856.7.h5" ;
:input_file371 = "2A21.20130418.87857.7.h5" ;
:input_file372 = "2A21.20130418.87858.7.h5" ;
:input_file373 = "2A21.20130418.87859.7.h5" ;
:input_file374 = "2A21.20130419.87860.7.h5" ;
:input_file375 = "2A21.20130419.87861.7.h5" ;
:input_file376 = "2A21.20130419.87862.7.h5" ;
:input_file377 = "2A21.20130419.87863.7.h5" ;
:input_file378 = "2A21.20130419.87864.7.h5" ;
:input_file379 = "2A21.20130419.87865.7.h5" ;
:input_file380 = "2A21.20130419.87866.7.h5" ;
:input_file381 = "2A21.20130419.87867.7.h5" ;
:input_file382 = "2A21.20130419.87868.7.h5" ;
:input_file383 = "2A21.20130419.87869.7.h5" ;
:input_file384 = "2A21.20130419.87870.7.h5" ;
:input_file385 = "2A21.20130419.87871.7.h5" ;
:input_file386 = "2A21.20130419.87872.7.h5" ;
:input_file387 = "2A21.20130419.87873.7.h5" ;
:input_file388 = "2A21.20130419.87874.7.h5" ;
:input_file389 = "2A21.20130420.87875.7.h5" ;
:input_file390 = "2A21.20130420.87876.7.h5" ;
:input_file391 = "2A21.20130420.87877.7.h5" ;
:input_file392 = "2A21.20130420.87878.7.h5" ;
:input_file393 = "2A21.20130420.87879.7.h5" ;
:input_file394 = "2A21.20130420.87880.7.h5" ;
:input_file395 = "2A21.20130420.87881.7.h5" ;
:input_file396 = "2A21.20130420.87882.7.h5" ;
:input_file397 = "2A21.20130420.87883.7.h5" ;
:input_file398 = "2A21.20130420.87884.7.h5" ;
:input_file399 = "2A21.20130420.87885.7.h5" ;
:input_file400 = "2A21.20130420.87886.7.h5" ;
:input_file401 = "2A21.20130420.87887.7.h5" ;
:input_file402 = "2A21.20130420.87888.7.h5" ;
:input_file403 = "2A21.20130420.87889.7.h5" ;
:input_file404 = "2A21.20130420.87890.7.h5" ;
:input_file405 = "2A21.20130421.87891.7.h5" ;
:input_file406 = "2A21.20130421.87892.7.h5" ;
:input_file407 = "2A21.20130421.87893.7.h5" ;
:input_file408 = "2A21.20130421.87894.7.h5" ;
:input_file409 = "2A21.20130421.87895.7.h5" ;
```

```
  :input_file410 = "2A21.20130421.87896.7.h5" ;
  :input_file411 = "2A21.20130421.87897.7.h5" ;
  :input_file412 = "2A21.20130421.87898.7.h5" ;
  :input_file413 = "2A21.20130421.87899.7.h5" ;
  :input_file414 = "2A21.20130421.87900.7.h5" ;
  :input_file415 = "2A21.20130421.87901.7.h5" ;
  :input_file416 = "2A21.20130421.87902.7.h5" ;
  :input_file417 = "2A21.20130421.87903.7.h5" ;
  :input_file418 = "2A21.20130421.87904.7.h5" ;
  :input_file419 = "2A21.20130421.87905.7.h5" ;
  :input_file420 = "2A21.20130422.87906.7.h5" ;
  :input_file421 = "2A21.20130422.87907.7.h5" ;
  :input_file422 = "2A21.20130422.87908.7.h5" ;
  :input_file423 = "2A21.20130422.87909.7.h5" ;
  :input_file424 = "2A21.20130422.87910.7.h5" ;
  :input_file425 = "2A21.20130422.87911.7.h5" ;
  :input_file426 = "2A21.20130422.87912.7.h5" ;
  :input_file427 = "2A21.20130422.87913.7.h5" ;
  :input_file428 = "2A21.20130422.87914.7.h5" ;
  :input_file429 = "2A21.20130422.87915.7.h5" ;
  :input_file430 = "2A21.20130422.87916.7.h5" ;
  :input_file431 = "2A21.20130422.87917.7.h5" ;
  :input_file432 = "2A21.20130422.87918.7.h5" ;
  :input_file433 = "2A21.20130422.87919.7.h5" ;
  :input_file434 = "2A21.20130422.87920.7.h5" ;
  :input_file435 = "2A21.20130422.87921.7.h5" ;
  :input_file436 = "2A21.20130423.87922.7.h5" ;
}
```